THE JOURNAL OF PHYSICAL CHEMISTRY C
A JOURNAL OF THE AMERICAN CHEMICAL SOCIETY

pubs.acs.org/JPCC

Article

Nonlinear Optical Responses from Au Surfaces as a Function of Temperature and Atmospheric Composition

Marshall T. McNally and Robert A. Walker*

Cite This: J. Phys. Chem. C 2022, 126, 17275−17282

Read Online

ACCESS | Metrics & More | Article Recommendations | Supporting Information

ABSTRACT: Second harmonic generation (SHG) was used to measure gold's second-order nonlinear optical response as a function of temperature and as a function of ambient atmosphere composition. Using a bespoke temperature-controlled assembly, SHG signal was measured from an Au surface between 19 and 260 °C under atmospheres containing varying amounts (0−100%) of O_2 with a balance of N_2. SHG intensity diminished with increasing temperature, a result that is interpreted in terms of increased electron−phonon scattering at higher temperatures. Surprisingly, SHG intensity also depended on ambient atmosphere, with the SHG signal measured in air (20% O_2) being ∼2 times larger than that measured in N_2 at room temperature. This dependence of SHG intensity on atmospheric composition disappeared at high temperatures. Systematically titrating O_2 into an N_2 feed showed that the room-temperature enhancement of SHG signal from Au saturated at ∼15% O_2. Despite widespread acceptance that O_2 does not adsorb to a bulk Au surface, we propose that these results are consistent with a weakly physisorbed surface excess of O_2 at the Au−gas interface. Fitting this O_2 enhancement of Au's SHG response to a Langmuir isotherm implies an adsorption energy on the order of 0.1 eV, consistent with results from previously reported DFT calculations. CO affects the SHG signal from Au in a manner similar to that of O_2, implying that the SHG enhancement is due to back-bonding of Au's conduction band electrons into vacant orbitals on either the O_2 or CO adsorbates.

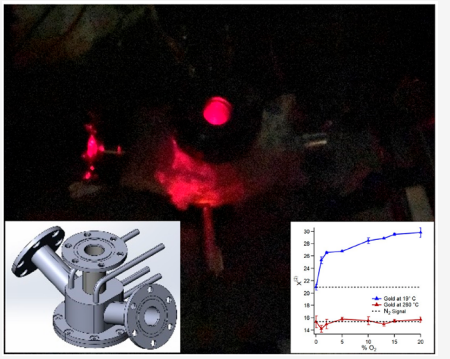

INTRODUCTION

For more than 40 years, second harmonic generation (SHG) has proven to be an invaluable technique for probing chemical structure and dynamics at interfaces. SHG is a second-order nonlinear optical method that, within the electric dipole approximation, is symmetry-forbidden in centrosymmetric media. As a result, a SH response only emerges when surface induced anisotropy leads to a break in inversion symmetry and corresponding nonzero elements in a molecule's or material's second-order susceptibility tensor, $\chi^{(2)}$. In addition to being surface-specific, SHG can also be species-specific as the resonant part of the $\chi^{(2)}$ tensor becomes large when either the incident light (at frequency ω) or the second harmonic signal (at 2ω) is resonant with allowed electronic transitions.[1] This surface and species selectivity has led to resonance-enhanced SHG being used to probe phenomena occurring at solid/vapor, solid/liquid, liquid/liquid, and liquid vapor interfaces.[2−8]

Conspicuously absent in the multitude of SHG studies, however, has been detailed consideration of how a system's SH response depends upon temperature, especially under ambient-pressure atmospheres and at elevated temperatures. This knowledge gap is particularly striking when considering the importance of electron−phonon scattering in materials and how electron−phonon scattering affects mass and thermal transport properties.[9] From a practical perspective, such information is directly relevant for any investigation using optical spectroscopy to study heterogeneous catalysis at elevated temperatures.[10,11] Time-dependent thermoreflectance measurements have reported that electron−phonon scattering (in bulk) increases with temperature and, in the limit of small electron perturbations, is dominated by nonthermal electrons, while larger perturbations resulting from higher intensity optical excitation show reduced contributions from the nonthermal population.[9] These experimental findings have been successfully modeled with time-dependent density functional theory (TD-DFT) where the authors reported that elevated temperatures accelerate electron−phonon scattering with higher frequency phonon modes coupling to the conducting electrons.[12]

Electron−phonon scattering should impact a material's second-order nonlinear response. SHG arises from a material's second-order polarization, $P^{(2)}$ and, consequently, depends quadratically on incident field strength ($E(\omega, t)$) and the second-order susceptibility:

Received: June 12, 2022
Revised: September 9, 2022
Published: October 3, 2022

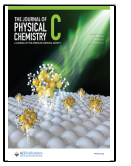

https://doi.org/10.1021/acs.jpcc.2c04065
J. Phys. Chem. C 2022, 126, 17275−17282

$$I(2\omega) \propto |P^{(2)}|^2 = |\chi^{(2)}|^2 |E(\omega, t)^2|^2 \quad (1)$$

where $\chi^{(2)}$ is the nonlinear susceptibility and $(I(2\omega))$ is the intensity of the SHG response. The nonlinear susceptibility is a third rank tensor containing 27 elements that can be separated into three groups: $\chi^{(2)}_{zxx} = \chi^{(2)}_{zyy}$, $\chi^{(2)}_{xxz} = \chi^{(2)}_{xzx} = \chi^{(2)}_{yyz} = \chi^{(2)}_{yzy}$, and $\chi^{(2)}_{zzz}$ In this frame of reference, x and y lie in the plane of the surface, and z projects along the surface normal. For a material, $\chi^{(2)}$ can also be written in terms of the frequency-dependent dielectric function (ε_ω) with respect to its surface contributions.

$$\chi^{(2)}_{\perp} \equiv a(\omega) \frac{e}{16\pi m\omega^2}(\epsilon_\omega - 1) \quad (2)$$

$$\chi^{(2)}_{\parallel} \equiv b(\omega) \frac{e}{16\pi m\omega^2}(\epsilon_\omega - 1) \quad (3)$$

$$\chi^{(2)}_{\text{bulk}} \equiv d(\omega) \frac{e}{16\pi m\omega^2}(\epsilon_\omega - 1) \quad (4)$$

where $a(\omega)$, $b(\omega)$, and $d(\omega)$ are dimensionless Rudnick−Stern parameters to account for surface conditions.[13,14] Room temperature measurements by Krause et al. showed $\chi^{(2)}_{\perp}$, later equated with the $\chi^{(2)}_{zzz}$, dominates the SHG response measured from a sputtered Au film, being ≥30 times larger than $\chi^{(2)}_{\parallel}$ and ∼1000 times larger than $\chi^{(2)}_{\text{bulk}}$.[15] Given the quadratic dependence of $I(2\omega)$ on $\chi^{(2)}$, these differences mean that the $I(2\omega)$ from $\chi^{(2)}_{\perp}$ will be ∼1000-fold and 10^6-fold larger than $I(2\omega)$ from $\chi^{(2)}_{\parallel}$ and $\chi^{(2)}_{\text{bulk}}$, respectively. Questions about the importance of quadrupolar contributions to the detected SH intensity[16−18] were addressed by Krause et al. by relating the bulk nonlinear current density to the nonlinear susceptibility to put an upper limit on $\chi^{(2)}_{\text{bulk}}$ relative to $\chi^{(2)}_{zzz}$,

In this treatment of a material's surface SHG response, temperature affects properties indirectly through the frequency-dependent, complex dielectric constant. The dielectric constant, ε_ω, depends upon the material's refractive index $(n(\omega))$ and extinction coefficient $(K(\omega))$ and the term $(\varepsilon_\omega - 1)$ is related directly to the material's optical conductivity (σ_ω) assuming a Drude model for an electron gas.[19]

$$\varepsilon_\omega = (n + iK)^2 \quad (5)$$

$$(\varepsilon_\omega - 1) = i\frac{4\pi}{\omega}\sigma_\omega \quad (6)$$

In this picture, conductivity is controlled by the electron scattering frequency (τ^{-1}):

$$\sigma_\omega = \frac{ne^2\tau}{m} \quad (7)$$

where n is the number of electrons, e is the electron charge, m is the electron mass, and τ is the scattering frequency of the sample's conduction band electrons. The temperature dependence in σ_ω comes from the temperature dependence in τ^{-1}. Parkins et al.[20] noted that the scattering frequency contains both a temperature *and* frequency dependence that could be represented as

$$\frac{1}{\tau} = \alpha(T) + \beta \times (\hbar\omega)^2 \quad (8)$$

where $\alpha(T)$ depends solely on electron−phonon scattering and β characterizes the electron−electron scattering. With these relationships, one can show that given fixed ω and 2ω, $\chi^{(2)}_{\perp}$ should diminish with increasing temperature according to the following expression

$$\chi^{(2)}_{\perp} \propto \frac{A}{\alpha(T) + B} \quad (9)$$

where A is a collection of constants and B is a constant arising from electron−electron scattering that depends upon ω and 2ω but *not* on temperature.[20] $\alpha(T)$ is calculated using a classical scattering model developed by Holstein.[21] In the work described below, experiments were carried out at temperatures well above gold's Debye temperature (178 K at room temperature) where electron−phonon scattering can be treated classically using the Wiedemann−Franz Law.[21] This description has been supported by studies showing that as the temperature increases, the imaginary part of the dielectric constant grows due to Drude broadening[22] or, equivalently, increased electron−phonon scattering. Spectroscopic ellipsometry experiments carried out with sputtered Au films show a doubling in the imaginary contribution to ε_ω, while the real contribution is insensitive to temperature over the temperature range relevant for studies reported in this work.[23]

As noted above, very few second-order nonlinear optical studies of materials at elevated temperatures have been reported. In one of the few studies of a material's nonlinear surface response at elevated temperatures, Shen and coworkers observed that the SHG signal from a (oxide-free) Si(111) surface decreased by ∼50% as the surface was heated (*in vacuo*) from 300 to 800 °C.[24] Results were reversible, and rather than attribute their observations to the material's dielectric properties, the authors assigned the change in the SHG response to temperature-dependent changes in Si(111)'s surface electronic states. In support of their interpretation, the authors noted that a native oxide layer on the Si(111) surface dampened this material's response almost quantitatively.

Experiments described below seek to quantify a simple material's temperature-dependent SHG response. The 100 nm sputtered Au film used in this work has cubic $Fm\bar{3}m$ space group symmetry and is centrosymmetric. We observe that the SHG response from Au is temperature-dependent with SH signal diminishing reversibly with increasing temperature. However, this effect is much more pronounced when O_2 is present compared to an inert (N_2 or Ar) atmosphere at ambient temperatures and disappears at temperatures ca. ≥200 °C. Very little difference in the Au's temperature-dependent SHG response was observed under air (20% O_2) versus pure O_2. We interpret the general SHG response, diminishing with increasing temperature, in terms of electron−phonon scattering, but the atmosphere-dependent discoveries suggest that Au's surface properties are influenced by *the gas phase composition above the surface*. This observation is surprising given that gases are generally considered rare media and unlikely to affect the properties of an adjacent condensed phase. Both thermal desorption studies and theory argue against molecular adsorption to the Au surface at these temperatures, although this assumption will need to be revisited in light of results presented below. In fact, the SHG results described in this work strongly suggest that at room temperature, an Au surface is covered by a weakly bound monolayer of physisorbed O_2.

EXPERIMENTAL SECTION

A 100 nm sputtered Au film (99.999%) was purchased from Sigma-Aldrich, cut into smaller pieces (∼1.5 × 1.5 cm), and used without modification except for repeated cleaning with methanol and water between experiments. Film thickness was

https://doi.org/10.1021/acs.jpcc.2c04065
J. Phys. Chem. C 2022, 126, 17275−17282

confirmed using a J. A. Woollam RC2 spectroscopic ellipsometer. The sample thickness was measured to be 103 ± 3 nm and the real and imaginary parts of the Au's reported dielectric constants compare favorably with literature (Figure 1A,B).[25,26] Temperature effects on crystal structure were

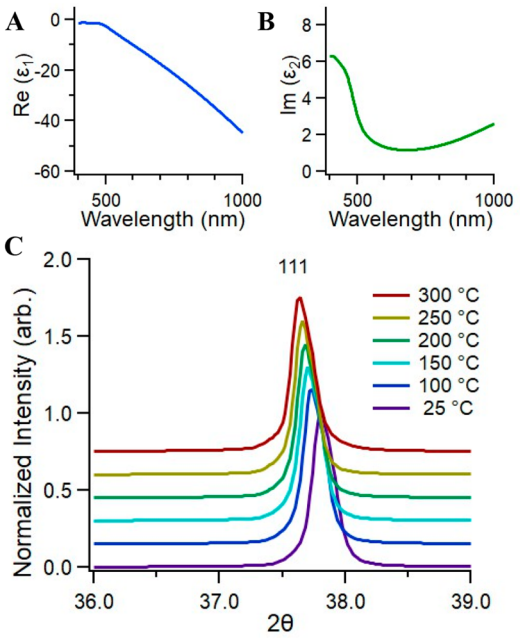

Figure 1. Real (a) and imaginary (b) portions of the dielectric function of gold. Temperature-dependent XRD of gold (c).

characterized with temperature-dependent X-ray diffraction (XRD) using a Rigaku Ultima IV. The sample was heated at 5 °C/min to 300 °C and cooled at the same rate, while taking a diffraction pattern was acquired every 50 °C. The XRD pattern (Figure 1C) show the expected peak shift due to thermal expansion of the lattice. The lattice constant was calculated to be 4.07 Å (Figure S1).

The SHG optical assembly used in these experiments has been described previously.[8,27] Briefly an amplified Ti:sapphire laser (800 nm, 85 fs pulse rate and 1 kHZ, ∼3.3 W) and directed into an optical parametric amplifier (Coherent Opera Solo) to produce 110 mW of 690 light. The incident light was attenuated to <2 mW using neutral density filters. A monochromator/photomultiplier tube assembly and photon counting electronics were used to detect the P-polarized SHG signal resulting from P-polarized incident light. This combination primarily sampled the $\chi^{(2)}_{zzz}$ (or $\chi^{(2)}_{\perp}$) tensor element.[15] Reported data have been background-corrected and normalized to incident power. Each measurement reflects the average of (at least) 3−6 independent measurements at each temperature.

SHG experiments were performed in a newly designed experimental assembly dubbed "Thermal Rig for OPtical Interfacial Characterization Spectroscopy (TROPICS)" (Figure 2). TROPICS consists of a two-piece sample housing and is equipped with three optical ports, two of which are angled at 67.5° from surface normal to enable concurrent reflectivity measurements and thermal imaging experiments as well as two gas ports, and two ports for experiments intended to examine a material's surface properties under electrochemical control

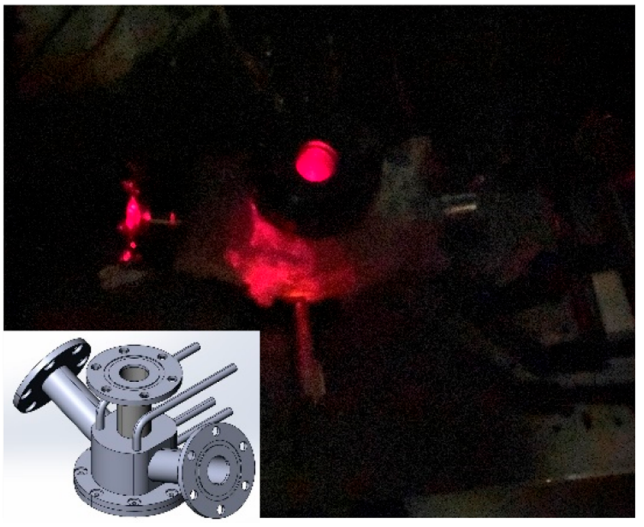

Figure 2. TROPICS at 456 °C with 690 nm incident light. 3D rendering of TROPICS design (insert).

For experiments described in this work, TROPICS was heated with heating tape (Duo-Tapes, HTS/Amptek) controlled by two LC-Z-120 switch controllers. A K-type thermocouple (Thermo-Scientific) was attached to the base plate and located ∼5 mm from the sample. Ambient atmospheres consisted of either bottled air, O_2 (99.997%), N_2 (99.999%), and chemically pure CO or Ar (99.999%). The chosen gas or gas mixture was flowed at 150 mm/min for single atmosphere experiments or 500 mm/min for binary mixture gas experiments, and TROPICS was allowed to equilibrate for 40 min whenever the composition was changed. At the start of an experiment, the sample was preheated to 260 °C at ∼2 °C/min to remove phyisorbed contaminants and then cooled (Figures S2 and S3). Once the sample returned to room temperature, the data acquisition began with SHG measurements being made in 30 °C increments up to 260 °C and then back down to test reversibility. We note that failure to begin with this heating−cooling cycle led to inconsistent results that were attributed to adventitious carbon on the surface. Repeated preheating/cooling cycles led to no changes to the data compared to a single heating/cooling cycle, and heating to higher temperatures (>300 °C) also had no further effect on the data.

RESULTS AND DISCUSSION

Gold's broad surface plasmon resonance (SPR) centered at ∼500 nm has made the material an attractive candidate to sensitize a host of optical measurements including surface enhanced Raman scattering,[28] fluorescence enhancement,[29] and second harmonic generation.[30] Experiments presented in this work measure the P-polarized SH response at 345 nm resulting from 690 nm P-polarized light incident on a 100 nm thick sputtered Au film as a function of temperature and of ambient atmosphere composition. Au's SHG response is modestly enhanced by the broad, blue edge of Au's SPR under these conditions. Temperature-dependent, normalized data acquired under air, N_2, O_2, and Ar atmospheres are shown in Figure 3.

Two general observations stand out in Figure 3. First, under all four atmospheres, the SH response decreases with increasing temperature and these changes are reversible.

https://doi.org/10.1021/acs.jpcc.2c04065
J. Phys. Chem. C 2022, 126, 17275−17282

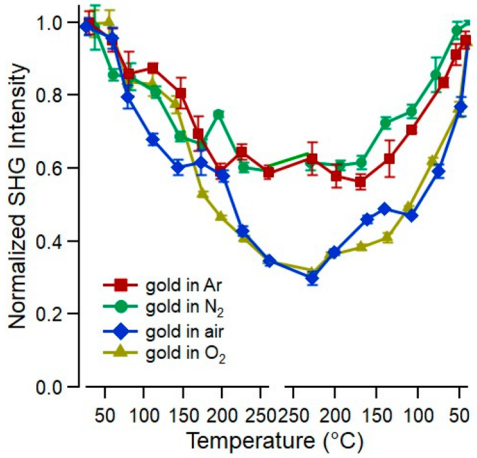

Figure 3. Normalized SHG response from sputtered gold surface under cylinder air (blue), ultrapure N_2 (99.999%) (green), ultrapure Ar (red), and ultrapure O_2 (gold) as a function of temperature.

Second, the magnitude of this response is much more pronounced for O_2 containing atmospheres relative to N_2 or Ar. These results and their significance are discussed below.

Signal Response versus Temperature. If one assumes that Au's conduction band electrons are responsible for the observed SHG signal, then $P^{(2)}$ induced by the incident field will diminish as the electron−phonon scattering frequency increases (see eqs 2 and 6−8). A simple description of electron−phonon scattering predicts that the scattering frequency, τ^{-1}, should increase between 50 and 70% as Au's temperature is raised from room temperature to 260 °C, the maximum experimental temperature reported in this study.[20,21] TD-DFT calculations performed by Prezhdo and co-workers predicted a 15% reduction in the dephasing time of electrons in thin Au films as the system temperature is raised from 100 to 300 K.[12] While a direct relationship between $P^{(2)}$ (and, by extension $\chi_{\perp}^{(2)}$) and electron−phonon scattering as a function of temperature is not straightforward to derive, the general dependence of $\chi_{\perp}^{(2)}$ on $\alpha(T)$ is reciprocal as shown in eq 9. The data shown in Figure 3 follow the behavior predicted by eq 9, noting that $\alpha(T)$ rises with temperature (reflecting increased electron phonon scattering rates). The 40% loss of signal observed for Au under inert atmospheres as the system temperature is raised from ambient to 260 °C requires that $\chi_{\perp}^{(2)}$ decreases by ∼20%.

Sources other than electron−phonon scattering may also contribute to the observed temperature-dependent change in Au's SHG response, but no single explanation can account for the observations reported in Figure 3. Tom et al. attributed the 50% reduction in Si(111)'s SHG signal as the system temperature was raised from room temperature to 800 °C to changes in surface electronic properties.[24] In the case of Au, however, this explanation seems unlikely given Au's overlapping valence and conduction bands. The hypothesis that Au's surface electronic properties are changing very little over this temperature range is supported by extensive temperature-dependent ellipsometry studies on Au thin films described by Reddy et al. that show almost no change in Au's optical properties in the wavelength region relevant to the SHG results described above.[25]

In principle, heating will reduce electron or carrier density in a material and, subsequently, reduce a material's $\chi^{(2)}$. Heating leads to lattice expansion. This reduction in free electron density is reflected in a decrease in the material's plasma frequency (ω_p) and a corresponding decrease in the real part of the material's complex dielectric constant. However, temperature-dependent XRD measurements (Figure 1C) have shown that over the temperature range sampled in this work, Au's lattice constant expands by ≤0.5%, making reduced electron density due to thermal expansion an unlikely source of SHG signal changes.

Finally, we considered that a temperature-dependent change in Au's SPR wavelength might be responsible for the observed loss in SHG intensity at higher temperatures. Yeshchenko et al. showed that Au's SPR shifts by ≤5 nm between room temperature and 260 °C.[31] Given the spectral line width of the transition and the 4 nm bandwidth of the laser pulse, such a shift should not contribute measurably to the observed SHG signal loss.

After considering all possible sources of signal loss, we attribute the temperature-dependent changes in SHG intensity from an Au surface to enhanced electron−phonon scattering. Data reported in Figure 3 are qualitatively consistent with predictions that have been advanced over the decades and can now be used to test different proposed scattering mechanisms.[32]

Signal Response versus Atmospheric Composition. A striking observation in Figure 3 is the effect of atmospheric composition on the magnitude of the temperature-dependent SHG response. For experiments carried out with inert atmospheres the Au SHG intensity drops by ∼40% over the temperature range sampled. Under O_2-containing atmospheres this change is 75% over the same temperature range. For all atmospheres, the observed changes are reversible with temperature and differences between O_2 containing atmospheres and inert (N_2 and Ar) atmospheres imply that molecular oxygen is either adsorbing or interacting with the Au surface in a way that measurably affects the material's second-order susceptibility.

In a recent review, Montemore et al. noted that molecular O_2 was the sole oxygen species that physisorbed to an Au surface.[33] (O_2 adsorption to other metal surfaces resulted in dissociative chemisorption and different oxide/peroxide/superoxide speciation.) However, molecular O_2 desorbs from Au at 55 K, meaning that the effects observed in Figure 3 do not reflect simple O_2 adsorption to form a stable monolayer.[34,35] Gas-surface scattering experiments found that most O_2 molecules scatter impulsively from Au surfaces with a very small amount (≤4%) of incident O_2 desorbing thermally with a Boltzmann velocity distribution.[36] Admittedly, the O_2 molecules in the scattering experiments collided with the Au surface with *hyperthermal* kinetic energies (5 eV) compared to the more modest *thermal* energies relevant in the SHG experiments (0.026−0.047 eV), but both the hyperthermal scattering experiments and results from thermal desorption studies consistently show that O_2 has a very low affinity for Au.

While direct comparisons with N_2 and Ar interacting with Au are difficult to make, studies of hyperthermal Ar scattering from graphite surfaces showed the importance of attractive interactions between the incident gas atom and the solid substrate in controlling the amount of energy transfer.[37] More recent results report a calculated interaction potential between Ar and Au of only ∼0.018 eV.[38] These values are small relative to O_2's calculated 0.10 eV adsorption energy to a Au (100) surface.[39] Similarly, DFT-based comparisons that calculate O_2

https://doi.org/10.1021/acs.jpcc.2c04065
J. Phys. Chem. C 2022, 126, 17275−17282

and N_2 interactions with a model Au film deposited on CaO (001) surfaces show O_2 to be ~2 times more attracted to the surface (D_e = 0.20 eV) than N_2 (0.09 eV).[40] In these calculations, results predict that the origin of this attraction is charge transfer from the Au to the O_2. No similar mechanism is predicted for N_2. Taken together, all of these results illustrate that while O_2 is not expected to interact strongly with a Au substrate, O_2's interactions are nevertheless stronger than those of N_2 or Ar.

Data in Figure 3 show that the atmosphere above the Au surface affects the surface's temperature-dependent SHG response, but the normalized intensities hide several important effects. Specifically, Figure 3 does not reveal whether the absolute SHG response under air is larger or smaller than the signal under N_2 at room temperature. Also absent is if/how the absolute intensities of the SHG response under air and N_2 differ at high temperatures. Figure 4 shows the square root of

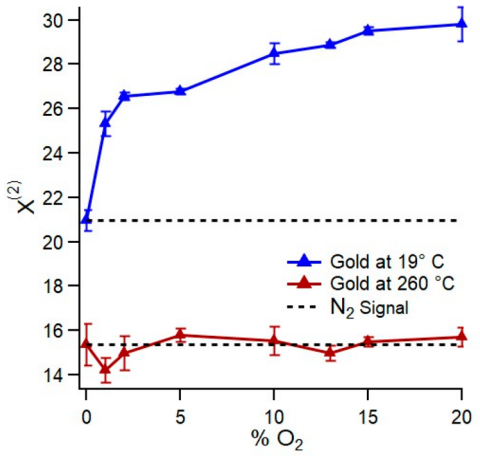

Figure 4. Change in nonlinear susceptibility of gold as a function of molecular oxygen concentration at 19 °C (blue) and 260 °C (red). Note that the *y*-axis now shows the square root of the measured SHG intensity, corresponding to the system's $|P^{(2)}|$. The 100% O_2 signal ≅ 20% O_2.

the SHG signal (= $\chi^{(2)}$) from Au as a function of %O_2 (with an N_2 balance) at 19 and 260 °C. The low temperature data reveal that $|\chi^{(2)}|$ does increase by ~50% with increasing O_2 content, saturating at ~15% O_2. At 260 °C, $|\chi^{(2)}|$ is invariant to O_2 content and equivalent to the material's response under pure N_2.

In light of this behavior, we propose that at ambient temperatures, O_2*weakly* physisorbs to Au, forming a loosely bound monolayer that saturates at 15% O_2. If the change in $|\chi^{(2)}|$ as a function of %O_2 reflects the number of physisorbed O_2 molecules, then the data in Figure 4 can be manipulated to account for surface coverage and fit to a Langmuir isotherm[41] (Figure 5).

$$\theta = \frac{Kp}{1 + Kp} \tag{10}$$

where K is an adsorption constant (in units of inverse pressure) and p is the O_2 partial pressure (taken to be equivalent to % O_2 as experiments are conducted at 1 atm total pressure). In this treatment, the $\chi^{(2)}$ data in Figure 4 first have subtracted the contribution from underlying Au substrate, assumed to be $\chi^{(2)}$ value under pure N_2. Then the data are

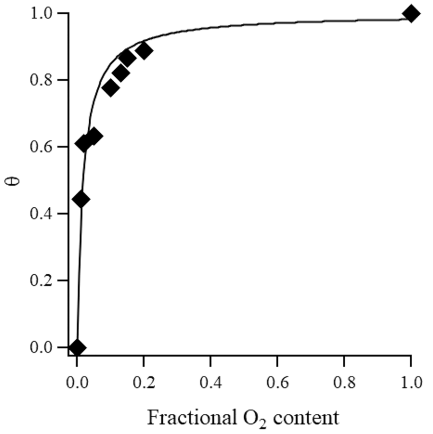

Figure 5. Langmuir isotherm fit to the $\chi^{(2)}$ enhancement as a function of O_2 content in the ambient atmosphere. Surface coverage data were derived from results in Figure 4 using the procedure described in the text.

normalized to value 100% O_2 and plotted versus fractional O_2 content.

While the fit does not perfectly capture the functional behavior at intermediate % O_2 compositions, it does a reasonable job of describing the overall observed trend. Furthermore, from the fitted adsorption constant (56), one calculates an adsorption energy of 0.10 eV at room temperature identical to the calculated 0.1 eV reported by Boronat and Corma.[39]

We note that this interpretation runs counter to the conventional view that O_2 does not adsorb to Au at ambient temperatures.[33] Instead, we view our results as being analogous to those describing soluble surfactant monolayer equilibrium at aqueous vapor interfaces, where the surfactant monomers themselves are constantly exchanging between the surface and bulk, and the surface coverage reflects a surface *excess* concentration relative to the bulk limit. This analogy is not perfect, but we believe the comparison has merit: Au is a rigid substrate with well-defined adsorption sites (compared to an aqueous-vapor interface), and O_2 "solutes" in the bulk are gas phase species with absolute number densities much lower than in condensed phase species. An attractive potential comparable to or greater than a gas particle's incident kinetic energy will localize excess O_2 at a surface. We propose that these O_2 molecules are the weakly physisorbed species that change the nonlinear response of the Au surface, and they are in constant exchange with the gas phase O_2. Higher temperatures ensure that any colliding O_2 molecule immediately acquires sufficient thermal energy to desorb, resulting in no surface excess and convergence in the high temperature limit to behavior observed for pure N_2.

A question remains about the mechanism responsible for O_2's enhancement of SHG from the Au surface at room temperature. Specifically, one might propose that the unpaired electrons responsible for O_2's paramagnetic properties increase the surface polarizability. N_2 with its more tightly bound electrons and closed shell configuration (and much weaker binding energy) would not to contribute to $\chi^{(2)}$ in any meaningful way. An alternative hypothesis is that an adsorbate on a Au surface enables electrons in the conduction band to delocalize through bonding/back-bonding into vacant orbitals on the adsorbate, thereby expanding their spatial distribution

https://doi.org/10.1021/acs.jpcc.2c04065
J. Phys. Chem. C 2022, 126, 17275−17282

and increasing the system's overall polarizability. This latter description is consistent with the charge transfer mechanism reported by Abdel Aal and co-workers.[40]

To test whether the larger SHG signal with O_2 was due to the weakly physisorbed O_2 or through enhanced nonlinear optical properties of the material itself, we conducted an experiment using 10% CO (in N_2). CO is isoelectronic with N_2 with all its electrons bound tightly in bonding orbitals. Unlike N_2, however, CO has a small dipole (0.12 D) and is an effective ligand because of its ability to accept electrons through the vacant π^* orbitals localized carbon monoxide's more positive carbon atom.

Figure 6 shows the normalized SHG signal from a Au surface as a function of temperature under atmospheres of air,

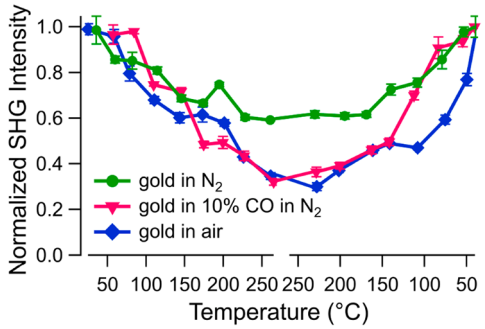

Figure 6. Normalized SHG response from sputtered gold surface under air (blue), ultrapure O_2 (gold) and 10% CO, UHP N_2 (light green) as a function of temperature. The air and N_2 data are equivalent to traces shown in Figure 3.

N_2, and 10% CO in N_2. The response of the CO system is virtually identical to that of Au under air, strongly supporting the hypothesis that the effects observed are due to physisorbed molecules enhancing the intrinsic response of the Au.

Similarities between the CO and air data in Figure 6 raise a host of interesting questions about the nature of the surface excess and how sensitive and accurate this experimental approach can be for experimentally determining gas-surface interaction potential. Hammer et al. used DFT to calculate CO chemisorption energies to Group 10 and 11 metals and found that these values ranged from −1.5 eV (CO to Pt) to +0.1 eV (CO to Ag).[42] (Here, a negative adsorption energy corresponds to an attractive potential.) Where comparisons could be made with experimental data, agreement was generally on the order of ±0.15 eV. (One exception is that the experimental chemisorption energy for CO on Ag has been reported as −0.28 eV.)[43] Using SHG to measure adsorption isotherms and binding energies will become more complicated in reactive systems where dissociative chemisorption effectively oxidizes the metal surface and no longer allows a reversible equilibrium to be established between the O_2 reservoir in the gas phase and a pristine metal surface. Nevertheless, the apparent sensitivity of this measurement to weakly adsorbed species points to a broad range of survey experiments that directly test predictions from theory.

A second line of inquiry that warrants further investigation is if changes in Au's $\chi^{(2)}$ resulting from O_2 (or CO) adsorption show evidence of new electronic resonances or if changes in phase of the different $\chi^{(2)}$ elements lead to apparent spectral features that are not reflective of new eigenstates. This latter issue is particularly relevant as interference between chemisorbed vibrational resonances, and the nonresonant part of gold's $\chi^{(2)}$ has often been used in vibrational sum frequency generation experiments to deduce the phase of *vibrational* $\chi^{(2)}$ contribution.[41,42,44−46] These considerations are complicated by needing to know Fresnel coefficients at three different frquencies (IR, visible, and sum). SHG measurements are easier to treat and work by Buck et al. showed how the SHG response from a Au substrate changed as an alkylthiol monolayer chemisorbed to the surface.[46]

Experiments reported by Buck et al. sampled a wavelength range of 615−670 nm (or a SHG window from 307 to 335 nm).[46] The authors noted that chemisorption led to an increase in $I(2\omega)$ but with a wavelength dependence showing a maximum in the monolayer/Au spectrum ∼650 nm (incident)/325 nm (SHG). Through careful measurements and separation of the different $\chi^{(2)}$ element amplitudes and phases, the authors attributed this observation to interferences that arose from the superposition of the different tensor elements and noted "...the spectral dependence of the tensor elements should be useful as a fingerprint of a given adsorbate−substrate system."[46] Results presented in the current work come from a system that is both similar to and profoundly different from the one studied by Buck et al. While both studies consider adsorbates affecting the nonlinear susceptibility of Au, the thiol monolayer studied by Buck et al. is covalently and irreversibly bound to the Au surface. In contrast, the O_2 adsorption reported in this work is weak and reversible. Dissecting how weakly physisorbed species affect individual elements in Au's $\chi^{(2)}$ tensor is a challenge that promises to resolve important questions about the chemical physics underpinning adsorption's effects on chemical properties.

CONCLUSION

Findings reported in this work address several important issues related to the surface properties of Au at elevated temperatures up to 260 °C and under ambient pressure atmospheres. First, temperature-dependent changes in the Au SHG response are consistent with predictions based on electron−phonon scattering, with increased scattering leading to a diminished second-order susceptibility. While this result is expected, it marks one of the few applications of SHG to high-temperature systems and the first attempt to correlate a materials surface electronic structure to the material's optical conductivity. Second, results show that Au's SHG response depends upon the adjacent gas phase composition. Specifically, gas phases containing O_2 have a larger effect on Au's second-order susceptibility at room temperature than inert atmospheres (such as N_2 or Ar). Oxygen's effect saturates at concentrations greater than 15% O_2 (in 1 atm). These effects disappear at higher temperatures such that the SHG responses from Au under air and under N_2 are equivalent at 260 °C. Collectively, these findings strongly suggest that in air at ambient pressure and room temperature, Au has a weakly physisorbed surface excess of O_2. This result stands in contrast to long-standing descriptions of O_2 interacting with bulk Au substrates with no reported surface affinity. Proof of principle measurements with CO show results similar to those with O_2 implying that donation from Au's conduction band electrons to the unfilled antibonding orbitals on O_2 and CO is responsible for the observed enhanced second-order susceptibility. The prospect of benchmarking SHG measurements of gas phase adsorption to metal surface at ambient pressures and temperatures is appealing and will be the subject of future studies.

https://doi.org/10.1021/acs.jpcc.2c04065
J. Phys. Chem. C 2022, 126, 17275−17282

■ ASSOCIATED CONTENT

Supporting Information

The Supporting Information is available free of charge at https://pubs.acs.org/doi/10.1021/acs.jpcc.2c04065.

Room-temperature XRD of Au(111), EDS of Au(111) surface, Auger spectra of Au (111) thermal cycled in TROPICS before and after sputtering with a 2 keV Ar ion beam (PDF)

■ AUTHOR INFORMATION

Corresponding Author

Robert A. Walker − *Montana Materials Science Program, Montana State University, Bozeman, Montana 59717, United States; Department of Chemistry and Biochemistry, Montana State University, Bozeman, Montana 59717, United States;* orcid.org/0000-0002-0754-6298; Email: rawalker@montana.edu

Author

Marshall T. McNally − *Montana Materials Science Program, Montana State University, Bozeman, Montana 59717, United States*

Complete contact information is available at: https://pubs.acs.org/10.1021/acs.jpcc.2c04065

Funding

This work was supported by the United States National Science Foundation. (CHE-1710695)

Notes

The authors declare no competing financial interest.

■ ACKNOWLEDGMENTS

The authors gratefully acknowledge Gary Wyss at Montana Technical University's Center for Metallurgical and Material Processing (CAMP) facility for assistance with temperature-dependent X-ray diffraction measurements. The authors also gratefully acknowledge Nida Shaikh for assistance with spectroscopic ellipsometry measurements.

■ REFERENCES

(1) Moad, A. J.; Simpson, G. J. A Unified Treatment of Selectrion Rules and Symmetry Relations for Sum-Frequency and Second Harmonic Generation. *Jounal of Physical Chemistry B* **2004**, *108*, 3548−3562.

(2) Campagnola, P.; Loew, L. Second-harmonic imaging microscopy for visualizing biomolecular arrays in cells, tissues and organisms. *Nat. Biotechnol.* **2003**, *21* (11), 1356−1360.

(3) Butet, J.; Brevet, P.-F.; Martin, O. Optical Second Harmonic Generation in Plasmonic Nanostructures: From Fundamental Principles to Advanced Applications. *ACS Nano* **2015**, *9* (11), 10545−10562.

(4) Hohlfeld, J.; Matthias, E.; Knorren, R.; Bennemann, K. H. Nonequilibrium Magnetization Dynamics of Nickel. *Phys. Rev. Lett.* **1997**, *78* (25), 4861−4864.

(5) Liu, S.; Sinclair, M.; Saravi, S.; Keeler, G.; Yang, Y.; Reno, J.; Peake, G.; Setzpfandt, F.; Staude, I.; Pertsch, T.; Brener, I. Resonantly Enhanced Second-Harmonic Generation Using III-V Semiconductor All dielectric Metasurfaces. *Nano Lett.* **2016**, *16*, 5426−5432.

(6) Wang, H.; Yan, E. C. Y.; Borguet, E.; Eisenthal, K. B. Second harmonic generation from the surface of centrosymmetric particles in bulk solution. *Chem. Phys. Lett.* **1996**, *259*, 15−20.

(7) Woods, L. B.; George, J. K.; Sherman, A. M.; Callis, P. R.; Walker, R. A. Adsorption and Aggregation at Silica/Methanol Interfaces: The Role of Solute Structure. *J. Phys. Chem. C* **2015**, *119*, 14230−14238.

(8) Purnell, G. E.; McNally, M. T.; Callis, P. R.; Walker, R. A. Buried Liquid Interfaces as a Form of Chemistry in Confinement: The Case of 4-Dimethylaminobenzonitrile at the Silica-Aqueous Interface. *J. Am. Chem. Soc.* **2020**, *142*, 2375−2385.

(9) Giri, A.; Gaskins, J. T.; Foley, B. M.; Cheaito, R.; Hopkins, P. E. Experimental evidence of excited electron number density and temperature effects on electron-phonon coupling in gold films. *J. Appl. Phys.* **2015**, *117*, 044305.

(10) Yin, M.; Yun, Z.; Fan, F.; Pillai, S. C.; Wu, Z.; Zheng, Y.; Zhao, L.; Wang, H.; Hou, H. Insights into the mechanism of low-temperature H_2S oxidation over Zn-Cu/Al_2O_3 catalyst. *Chemosphere* **2022**, *291*, 133105.

(11) Ullattil, S. G.; Narendranath, S. B.; Pillai, S. C.; Periyat, P. Black TiO_2 Nanomaterials: A Review of Recent Advances. *Chemical Engineering Journal* **2018**, *343*, 708−736.

(12) Zhou, X.; Li, L.; Dong, H.; Giri, A.; Hopkins, P. E.; Prezhdo, O. V. Temperature Dependence of Electron-Phonon Interactions in Gold Films Rationalized by Time-Domain Ab Initio Analysis. *J. Phys. Chem. C* **2017**, *121*, 17488−17497.

(13) Murphy, R.; Yeganeh, M.; Song, K. J.; Plummer, E. W. Second-Harmonic Generation from the Surface of a Simple Metal, Al. *Phys. Rev. Lett.* **1989**, *63* (3), 318−321.

(14) Janz, S.; Pedersen, K.; van Driel, H. M.; Timsit, R. S. Structural Transformations in Adsorbed Oxygen Layers on Al Surfaces Observed Using Optical Second-Harmonic Generation. *Journal of Vacuum Science & Technology A* **1991**, *9* (3), 1506−1510.

(15) Krause, D.; Teplin, C. W.; Rogers, C. T. Optical Surface Second Harmonic Measurements of Isotropic Thin Film Metals: Gold, Silver, Copper, Aluminum and Tantalum. *J. Appl. Phys.* **2004**, *96* (7), 3626−3634.

(16) Reitböck, C.; Stifter, D.; Alejo-Molina, A.; Hingerl, K.; Hardhienata, H. Bulk Quadrupole and Interface Dipole contribution for Second Harmonic Generation in Si(111). *J. Opt.* **2016**, *18*, 035501.

(17) Farenbruch, A.; Mund, J.; Fröhlich, D.; Yakovlev, D. R.; Bayer, M.; Semina, A.; Glazov, M. M. Magneto-Stark and Zeeman Effect as Origin of Second Generation of Excitons in Cu_2O. *Phys. Rev. B* **2020**, *101*, 1115201.

(18) Timpu, F.; Sergeyev, A.; Hendricks, N. R.; Grange, R. Second-Harmonic Enhancement with Mie Resonances in Perovskite Nanoparticles. *ACS Photonics* **2017**, *4*, 76−84.

(19) Kittel, C. Chapter 15. In *Introduction to Solid State Physics*, 8th ed.; John Wiley and Sons, 2005.

(20) Parkins, G. R.; Lawrence, W. E.; Christy, R. W. Intraband Optical Conductivity $\sigma(\omega,T)$ of Cu, Ag and Au: Contribution from Electron-Electron Scattering. *Phys. Rev. B* **1981**, *23* (12), 6408−6416.

(21) Holstein, T. Theory of Transport Phenomena in an Electron-Phonon Gas*. *Annals of Physics* **1964**, *29*, 410−535.

(22) Reddy, H.; Guler, U.; Chaudhuri, K.; Dutta, A.; Kildishev, A. V.; Shalaev, V. M.; Boltasseva, A. Temperature-Dependent Optical Properties of Single Crystalline and Polycrystalline Silver Thin Films. *ACS Photonics* **2017**, *4*, 1083−1091.

(23) Reddy, H.; Guler, U.; Kudyshev, Z.; Kildishev, A. V.; Shalaev, V. M.; Boltasseva, A. Temperature-Dependent Optical Properties of Plasmonic Titanium Nitride Thin Films. *ACS Photonics* **2017**, *4*, 1413−1420.

(24) Tom, H. W. K.; Zhu, X. D.; Shen, Y. R.; Somorjai, G. A. Investigation of the Si(111)-(7 × 7) Surface By Second-Harmonic Generation: Oxidation and the Effects of Surface Phosphorus. *Surf. Sci.* **1986**, *167*, 167−176.

(25) Reddy, H.; Guler, U.; Kildishev, A. V.; Boltasseva, A.; Shalaev, V. M. Temperature-Dependent Optical Properties of Gold Thin Films. *Optical Materials Express* **2016**, *6* (9), 2776−2802.

(26) Olmon, R. L.; Slovick, B.; Johnson, T. W.; Shelton, D.; Oh, S.; Boreman, G. D.; Raschke, M. B. Optical Dielectric Function of Gold. *Phys. Rev. B* **2012**, *86* (23), 235147.

(27) Purnell, G. E.; Walker, R. A. Surface Solvation and Hindered Isomerization at the Water/Silica Interface Explored with Second Harmonic Generation. *J. Chem. Phys.* **2019**, *150*, 194701.
(28) Ding, S.-Y.; Yi, J.; Li, J.-F.; Ren, B.; Wu, D.-Y.; Panneerselvam, R.; Tian, Z.-Q. Nanostructure-Based Plasmon Enhanced Raman Spectroscopy for Surface Analysis of Materials. *Nat. Rev. Mater.* **2016**, *1*, 16021.
(29) Saha, K.; Agasti, S. S.; Kim, C.; Li, X.; Rotello, V. M. Gold Nanoparticles in Chemical and Biological Sensing. *Chemistry Reviews* **2012**, *112*, 2739−2779.
(30) Czaplicki, R.; Kiviniemi, A.; Huttunen, M. J.; Zang, X.; Stolt, T.; Vartiainen, I.; Butet, J.; Kuittinen, M.; Martin, O. J. F.; Kauranen, M. Less Is More: Enhancement of Second-Harmonic Generation from Metasurfaces by Reduced Nanoparticle Density. *Nano Lett.* **2018**, *18*, 7709−7714.
(31) Yeshchenko, O. A.; Bondarchuk, I. S.; Gurin, V. S.; Dmitruk, I. M.; Kotko, A. V. Temperature Dependence of the Surface Plasmon Resonance in Gold Nanoparticles. *Journal of Surface Science* **2013**, *608*, 275−281.
(32) Beach, R. T.; Christy, R. W. Electron-Electron Scattering in the Intraband Optical Conductivity of Cu, Ag, and Au. *Phys. Rev. B* **1977**, *16* (15), 5277−5284.
(33) Montemore, M. M.; van Spronsen, M. A.; Madix, R. J.; Friend, C. M. O_2 Activation by Metal Surfaces: Implications for Bonding and Reactivity on Heterogeneous Catalysts. *Chemistry Review* **2018**, *118*, 2816−2862.
(34) Gottfried, J. M.; Schmidt, K. J.; Schroeder, S. L. M.; Christmann, K. Spontaneous and Electron-Induced Adsorption of Oxygen on Au(110)-(1 × 2). *Surf. Sci.* **2002**, *511*, 65−82.
(35) Yan, M.; Huang, Z.-Q.; Zhang, Y.; Chang, C.-R. Trends in water-promoted oxygen dissociation on the transition metal surfaces from first principles. *Phys. Chem. Chem. Phys.* **2017**, *19*, 2364−2371.
(36) Murray, V. J.; Pilinski, M. D.; Smoll, E. J., Jr; Qian, M.; Minton, T. K.; Madzunkov, S. M.; Darrach, M. R. Gas-Surface Scattering Dynamics Applied to Concentration of Gases for Mass Spectrometry in Tenuous Atmospheres. *J. Phys. Chem. C* **2017**, *121*, 7903−7922.
(37) Gibson, K. D.; Sibener, S. J.; Upadhyaya, H. P.; Brunsvold, A. L.; Zhang, J.; Minton, T. K.; Troya, D. Hyperthermal Ar Atom Scattering from a C(0001) Surface. *J. Chem. Phys.* **2008**, *128*, 224708.
(38) Grenier, R.; To, Q.-D.; de Lara-Castells, M. P.; Léonard, C. Argon Interaction with Gold Surfaces: *Ab initio*-Assisted Determination of Pair Ar-Au Potentials for Molecular Dynamics Simulations. *J. Phys. Chem. A* **2015**, *119*, 6897−6908.
(39) Boronat, M.; Corma, A. Oxygen Activation on Gold Nanoparticles: Separating the Influence of Particle Size, Particle Shape and Support Interaction. *Dalton Transactions* **2010**, *39*, 8538−8546.
(40) Abdel Aal, S. A.; Shalabi, A.S.; Halim, W.S. A. Interaction of O_2 and N_2 Molecules with Au Deposited on Regular and Defective CaO (001) Surfaces: Density Functional Calculations. *Thin Solid Films* **2013**, *545*, 341−352.
(41) Swenson, H.; Stadie, N. P. Langmuir's Theory of Adsorption: A Centennial Review. *Langmuir* **2019**, *35* (16), 5409−5426.
(42) Hammer, B.; Morikawa, Y.; Nørskov, J. K. CO Chemisorption at Metal Surfaces and Overlayers. *Phys. Rev. Lett.* **1996**, *76* (12), 2141−2144.
(43) McElhiney, G.; Papp, H.; Pritchard, J. The Adsorption of Xe and CO on Ag(111). *Surf. Sci.* **1976**, *54*, 617−634.
(44) Cimatu, K.; Baldelli, S. Sum Frequency Generation Microscopy of Microcontact-Printed Mixed Self-Assembled Monolayers. *J. Phys. Chem. B* **2006**, *110*, 1807−1813.
(45) Dreesen, L.; Humbert, C.; Celebi, M.; Lemaire, J. J.; Mani, A. A.; Thiry, P. A.; Peremans, A. Influence of the Metal Electronic Properties on the Sum-Frequency Generation Spectra of Dodecanethiol Self-Assembled Monolayers on Pt (111), Ag (111) and Au (111) Single Crystals. *Appl. Phys. B: Laser Opt.* **2002**, *74*, 621−625.
(46) Buck, M.; Eisert, F.; Grunze, M.; Träger, F. Second-Order Nonlinear Susceptibilities of Surfaces. *Appl. Phys. A: Mater. Sci. Process.* **1995**, *60*, 1−12.

https://doi.org/10.1021/acs.jpcc.2c04065
J. Phys. Chem. C 2022, 126, 17275−17282